Electrocorticography and stereo EEG provide distinct measures of brain connectivity: Implications for network models

John M. Bernabei[1,2], T. Campbell Arnold[1,2], Preya Shah[1,2], Andrew Revell[1,2], Ian Z. Ong[1,2], Lohith G. Kini[1,2], Joel M. Stein[3], Russell T. Shinohara[4,5,6], Timothy H. Lucas[7], Kathryn A. Davis[2,8], Danielle S. Bassett[1,7,8,9,10,11,12], Brian Litt[1,2,7,8]

Affiliations:

[1]Department of Bioengineering, University of Pennsylvania, Philadelphia, PA, 19104
[2]Center for Neuroengineering & Therapeutics, University of Pennsylvania, Philadelphia PA 19104
[3]Department of Radiology, Hospital of the University of Pennsylvania, Philadelphia, PA, 19104
[4]Department of Biostatistics, Epidemiology, & Informatics, University of Pennsylvania, Philadelphia, PA, 19104
[5]Statistics in Imaging and Visualization Center, University of Pennsylvania, Philadelphia, PA, 19104
[6]Center for Clinical Epidemiology and Biostatistics, University of Pennsylvania, Philadelphia, PA, 19104
[7]Department of Neurosurgery, Hospital of the University of Pennsylvania, Philadelphia, PA, 19104
[8]Department of Neurology, Penn Epilepsy Center, Hospital of the University of Pennsylvania, Philadelphia, PA, 19104 USA
[9]Department of Electrical & Systems Engineering, University of Pennsylvania, Philadelphia, PA, 19104
[10]Department of Physics & Astronomy, University of Pennsylvania, Philadelphia, PA, 19104
[11]Department of Psychiatry, University of Pennsylvania, Philadelphia, PA, 19104
[12]The Santa Fe Institute, Santa Fe, NM, 87501

To whom correspondence should be addressed: John.Bernabei@pennmedicine.upenn.edu

Word counts (excluding figure captions):
Abstract: 224

Introduction: 981
Methods: 1139
Results: 1246
Discussion: 1795

Total: 5161 (excluding abstract)

Number of tables: 1
Number of figures: 4

Abstract:

Brain network models derived from graph theory have the potential to guide functional neurosurgery, and to improve rates of post-operative seizure freedom for patients with epilepsy. A barrier to applying these models clinically is that intracranial EEG electrode implantation strategies vary by center, region and country, from cortical grid & strip electrodes, to purely stereotactic depth electrodes, to a mixture of both. To determine whether models derived from one type of study are broadly applicable to others, we investigate the differences in brain networks mapped by electrocortiography (ECoG) and stereoelectroencephalography (SEEG) in a matched cohort of patients who underwent epilepsy surgery. We show that ECoG and SEEG map broad network structure differently, and demonstrate substantial disparity in the ability of node strength to localize the epileptogenic zone in SEEG compared to ECoG. We demonstrate that eliminating white matter contacts and reducing network nodes to anatomical regions of interest rather than individual contacts improves the ability of these models to distinguish between epileptogenic and non-epileptogenic regions in SEEG. Our findings suggest that effectively applying computational models to localize epileptic networks requires accounting for the effects of spatial sampling, particularly when analyzing both ECoG and SEEG recordings in the same cohort. Finally, we share all code and data in this study, aiming for our findings to accelerate research in brain network connectivity in epilepsy and beyond.

Keywords: epilepsy, intracranial EEG, functional connectivity, brain network model

1. Introduction:

Intracranial electrode recordings from patients with medically-refractory epilepsy characterize the brain's local function, widespread network organization, and guide surgical therapy. From the earliest days of intracranial EEG (iEEG), two major approaches have been used by clinicians for these purposes. In North America, Penfield's use of subdural grid and strip electrodes for electrocorticography (ECoG) persists at many major centers now decades after its initial use[1,2]. Meanwhile, centers in France and Italy still favor Talaraich and Bancaud's approach of using purely depth electrodes in stereoelectroencephalography (SEEG) pioneered at St. Anne's Hospital in Paris[2,3]. Recently, many centers that had used ECoG in the United States have changed to SEEG, due to its superior risk profile and tolerability, though some centers continue to favor ECoG, due to its superior cortical spatial coverage[4]. Unfortunately, many patients do not become seizure free after epilepsy surgery, regardless of implant technique. The reasons for this are unclear, but it is likely in part because the interpretation of intracranial recordings is complex, subjective, and plagued by sampling uncertainty[5]. It is also difficult to determine where and how much of the epileptic network must be resected or ablated to fully prevent seizures, particularly in cases where there are no obvious lesions on MRI[6]. Validated, quantitative methods to guide epilepsy surgery could lead to a greater rate of seizure freedom and greater clinical benefit to patients.

Recent evidence supports the hypothesis that epilepsy arises from disordered connectivity[7,8], and that mapping brain networks may aid in both selecting candidates for invasive treatment and identifying therapeutic targets for surgical resection, ablation or device implants. In a brain network model, discrete 'nodes' exist either at the sensor-level for functional connectivity derived from iEEG signals, or at the atlas region-of-interest (ROI) level for structural connectivity

derived from imaging[9]. Edges quantify the statistical relationships between nodes in functional connectivity approaches, or streamline count derived from DTI in structural connectivity. A variety of network methods are being explored to localize the epileptogenic zone from intracranial EEG data. Such approaches use interictal[10–13] or ictal recordings[14–16] and are derived from ECoG[10,11,14] or SEEG[17,18] to generate networks. These networks are analyzed using graph theory[10,14,19] or neural mass models, which simulate seizure-like activity and probe the effects of different surgical interventions[11,13]. Intracranial EEG network models are also used to study networks activated during normal brain function, for example in recent studies probing cognition[20] and attention[21]. The majority of these studies use patients implanted with ECoG, often supplemented with depth electrodes placed in the hippocampus. Unfortunately, because of the lack of standardization and difficulties in sharing iEEG data across centers, exceedingly few studies test their methods in both ECoG and SEEG. In order to validate and translate network methods into clinical practice across centers, it is important to understand how these variations in electrode implantation impact estimate connectivity, subsequent network models and their clinical utility.

While networks derived from brain images easily generalize across patients and centers due to congruence in their full-brain spatial sampling, iEEG functional networks suffer from sparse sampling and implant heterogeneity. Still, the problem of spatial sampling bias which affects iEEG networks[22] may be offset by: (1) the superior spatiotemporal resolution of iEEG in implanted regions, compared to functional neuroimaging and (2) experience that associates particular patterns in the EEG with typical onset regions, though it can sometimes be difficult to tell if these patterns are the result of seizure generation or spread. To better translate network models into patient care, we must better understand the extent of bias or sensitivity introduced by electrode implantation strategy, in this case ECoG versus SEEG, and its effect on network models. We must

then either change implant strategy or develop computational methods to correct for this effect. It is important to note that tradition in specific centers is not the only thing that guides choice of electrode implantation strategy. Other issues, such as the need for stimulation mapping, characteristics of a lesion such as its type and location, ictal semiology and suspected clinical syndrome, as well surgeon and epileptologist experience and training may also factor into approach and electrode choice[23].

There are many differences in implantation strategy between ECoG and SEEG that arise from the electrode hardware itself. Patients implanted with a large ECoG grid will have regular spacing between contacts in the same electrode (e.g. an 8x8 contact grid), supplemented with a few additional strip and depth electrodes in other regions, as needed. The implantation strategy is much more heterogeneous in SEEG. This heterogeneity can manifest itself in the following ways: (i) a wide range in the number of depth electrodes & electrode contacts from center to center, (ii) different spatial orientations and density of depth electrode implantation, (iii) different assortments of anatomical targets, electrode spacing and (iv) different levels of implant bilaterality[4]. Thus, translating network models into clinical care faces the challenge not only of resolving differences between ECoG and SEEG approaches, but also a high variability in SEEG approaches from center to center. It is unclear whether these distinct properties of electrodes and implant strategy preferentially degrade network representations derived from one approach vs the other, and whether they preclude using the same analysis for networks derived from SEEG and ECoG.

In this study, we explore the effect of implantation strategy, ECoG vs. SEEG, in patients with drug-resistant epilepsy being evaluated for invasive treatment. We use a balanced sample of both ECoG and SEEG patients matched as closely as possible for primary targets, clinical outcome, and lesional status. We hypothesize the following: (i) sampling differences between

ECoG and SEEG image distinct network properties and (ii) that different properties of the epileptogenic zone, as measured by these techniques, will degrade the performance of network models validated for ECoG when applied to SEEG. We aim for our findings to help translate personalized network models of epilepsy into clinical practice, and to inform analyses for other neuroscience and clinical applications.

2. Methods:

2.1 Patient data acquisition

We retrospectively analyzed a data set consisting of 60 patients who underwent intracranial recording during evaluation for epilepsy surgery, 55 of whom underwent surgery at the Hospital of the University of Pennsylvania (HUP) and five at the Mayo Clinic. Twenty-seven of these patients were implanted with grid, strip, and a small number of depth electrodes, comprising the ECoG group, while the remaining patients were implanted with only stereotactically placed depth electrodes: the SEEG group. All patients underwent either resection or laser ablation after electrode explant. Table 1 lists specific subject demographics in detail. We attempted to match cohorts for surgical targets and seizure outcome as closely as possible. Matching groups for surgical procedure was not possible, given the preponderance of laser ablations performed following the switch to SEEG at HUP. All subjects provided consent to have their full-length intracranial EEG recordings and anonymized imaging and metadata publicly released on the ieeg.org portal, an open-source online repository for electrophysiologic studies[24,25].

Each patient underwent a standard epilepsy imaging protocol including pre-implant MRI, post implant CT, and post-resection MRI. Patients at HUP also received post-implant MRI. We have previously described our method for localizing electrode locations in detail[14,26], and briefly summarize them in Figure 1. Post-iEEG-implant MRI (Figure 1D) is registered to pre-implant

	ECoG	SEEG	p-value
Total number of subjects	27	33	
Surgical outcome			0.80[a]
Good (Engel I)	18	23	
Poor (Engel II+)	9	10	
Resected / Ablated region			0.37[a]
Temporal	19	20	
Frontal/Parietal	8	10	
Insular	0	2	
MRI*			0.93[a]
Lesional	9	14	
Non-Lesional	11	18	
Type of surgery			4.8e-5[a]
Resection	23	11	
RF ablation	4	22	
Node counts			
Total			
Mean ± std. dev.	83.6 ± 28.1	119.6 ± 42.2	0.0015[b]
White matter			
Mean ± std. dev.	2.7 ± 3.4	29.6 ± 12.7	4.4e-11[b]
Resected / ablated			
Mean ± std. dev.	15.7 ± 12.8	9.2 ± 6.2	0.028[b]

Table 1: Clinical and demographic information. We analyzed a retrospective cohort of 60 patients with drug-resistant epilepsy who underwent surgery. Abbreviations: LTL - left temporal lobe, RTL – right temporal lobe, LFL – left frontal lobe, LFPL – left frontoparietal lobe, RFL – right frontal lobe, RFPL – right frontoparietal lobe. *We were unable to obtain the radiology report for some ECoG patients from the Mayo clinic. [a] = Chi-square test of proportion; [b] = Wilcoxon rank-sum test.

MRI (Figure 1C) and electrodes are segmented to derive their coordinates using ITK-SNAP[27]. We then registered the pre-implant MRI into Montreal Neurological Institute (MNI) space for use with neuroimaging atlases. We chose the AAL-116 atlas[28] to assign each electrode contact location a brain region of interest (ROI). Finally, we used a semi-automated algorithm previously described and validated[14] to perform resection and ablation zone segmentations, which allow the electrode contacts targeted by surgery to be determined. Information on the total number of electrode contacts, the number of contacts targeted, and the number of contacts lying in white matter are also listed in Table 1, and additional patient-level

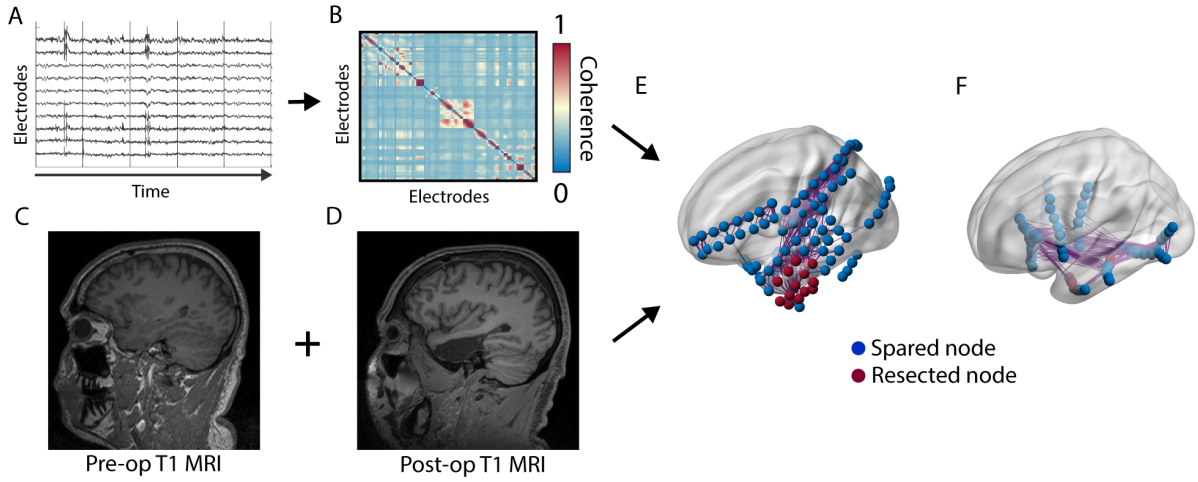

Figure 1. Imaging and network methods: (A) We use artifact-free clips of interictal iEEG to calculate (B) mean adjacency matrices using multitaper coherence. (C) Pre-operative and (D) post-operative T1 weighted MRI are used to segment the resection cavity which is used to determine resected nodes. (E) Together, we construct networks with the resected nodes determined in ECoG. (F) SEEG implantations using only depth electrodes appear distinct even for similar anatomic targets.

metadata may be found in supplemental table 1.

2.2 Connectivity calculation

We calculated functional connectivity using a pipeline that we have previously described and validated[10,14,16]. We used intracranial EEG stored on ieeg.org, a cloud-based platform for electrophysiologic data[24,25]. We randomly selected an interictal segment of > 2 minutes for each patient that occurs at least 1 hour away from clinically-annotated seizures; the segment length is justified by prior evidence that even short interictal segments accurately capture critical network patterns in epilepsy[29]. We divided the interictal epoch into one-second intervals (Figure 1A) and for each window calculated connectivity using coherence in the beta (15-40 Hz) band, which we have previously shown to be effective at detecting abnormal connectivity[10]. We computed the mean of each edge over time to obtain a single adjacency matrix for each patient (Figure 1B). Together with the results of our imaging pipeline, this process yielded networks in which each

node is either resected/ablated or spared in both patients with ECoG (Figure 1E) and SEEG (Figure 1F).

2.3 Network methods

To probe each network's structure we detected communities using modularity maximization, which labels nodes so that each community is comprised of nodes that are more connected to each other and relatively less connected to all other nodes outside of their community[30]. We used the Louvain method to maximize the following modularity quality index $Q = \frac{1}{2m}\sum_{ij}\left[A_{ij} - \frac{k_i k_j}{2m}\right]\delta(c_i c_j)$, where A_{ij} is link between nodes i and j, k are edge weights, m is the sum of all edge weights in the graph, and δ is the Kronecker delta function. To compare community structure across patients, we computed the participation coefficient[31] which measures the ratio of a node's connectivity strength external versus internal to its module. Averaging participation coefficient across nodes within each patient yielded an estimate of whether networks are (i) integrated, with high connectivity between modules, or (ii) segregated, with lower connectivity between modules.

We also assessed the extent to which networks in ECoG and SEEG have small-world properties, which is a property of networks that can support the efficient flow of information. The small-world property is well documented in biological networks such as those found in the brain and can be defined as the ratio of an appropriately normalized clustering coefficient to an appropriately normalized path length[32]. High values of the small-world index imply that a network has dense local connectivity structure yet can efficiently spread information elsewhere through topologically long-distance connections across the network. Here, we used the more precise formulation of the small-world propensity (SWP) which is adapted to better characterize the small-world property in weighted networks; it measures the clustering coefficient and path length

normalized to those calculated from random and lattice network null models that contain the same number of nodes and display the same edge weight distributions as the real network[33].

To illustrate the importance of differences in the way ECoG and SEEG represent epileptic networks in-vivo, we compared the ability of connectivity derived from these modalities to localize the epileptogenic zone. We chose the simple network metric of node strength, computed as the sum of all edge weights connecting it to all other nodes and is computed as $s_i = \sum_{j=1}^{N} A_{ij}$ in which s_i is the strength of node i, A_{ij} is the adjacency matrix element containing the edge weight between node j and node i, and N is the number of nodes. Our group has previously demonstrated that high node strength localizes the epileptogenic zone and predicts surgical outcome in patients implanted with ECoG[10,19], however its translatability to SEEG is unknown.

2.4 Statistical Approach

In our comparisons of network properties between ECoG and SEEG groups we primarily used nonparametric statistical tests such as the Wilxocon rank-sum test, as they do not assume that data are normally distributed. To assess the ability for node strength to detect epileptogenic regions, we use a metric known as the distinguishability statistic (D_{rs}) which quantifies the area under the receiver operating characteristic curve for classifying nodes as either resected or non-resected[29]. The quantity D_{rs} has been previously studied and validated for its ability to quantify whether networks have sufficient information to determine resected or non-resected regions[29]. This value is equivalent calculated as the normalized U-statistic, and ranges from 0-1. In our study, a value of 1 implies that all EZ nodes are higher in strength than all non-resected nodes; a value of 0 means that all EZ nodes are weaker than all non-resected nodes; and a value of 0.5 implies that node strength is unable to distinguish the epileptogenic zone.

2.5 Data-sharing

One of our primary goals is to aid in the translation of epilepsy network models into clinical practice. To this end, we share all raw intracranial EEG and imaging data for HUP patients at iEEG.org, a free cloud sharing platform for electrophysiological data in the folder HUP_Intracranial_Data. The code for calculating adjacency matrices is available at GitHub.com/Akhambhati/echobase, processed adjacency matrices, and code for comparing networks between ECoG and SEEG is hosted at GitHub.com/jbernabei/ecog_vs_seeg.

3. Results:

We first compare networks mapped by ECoG and SEEG in a cohort of matched epilepsy patients. We aim to describe how each approach is biased towards characteristic patterns of anatomical electrode distributions which lead to distinct network properties. We then compare how these distinct network properties affect how well connectivity can distinguish epileptogenic and non-epileptogenic regions with the ultimate goal of improved surgical planning.

3.1 Anatomical sampling differs greatly across modalities

We first asked what differences exist between ECoG and SEEG in quantity of electrodes implanted in different regions. After quantifying the top 15 anatomical targets (Figure 2A), we found that a greater number of top targets in SEEG are contralateral to the ultimate epileptogenic zone (ranks 6, 9, 13, 15) compared to ECoG, whereas targets contralateral to seizure onset do not comprise any of the most sampled regions in ECoG. This finding indicates that SEEG, at our center, typically gives a broader representation of the brain as a whole, compared to ECoG. This finding confirms that in our cohort ECoG has greater cortical representation in the hemisphere of the resection zone. While this finding makes sense in that bilateral ECoG grids are rarely placed, due to potential morbidity, unilateral grids can be safely paired with contralateral subdural strips or depth electrodes placed through burr holes, if indicated. We then sought to quantify the

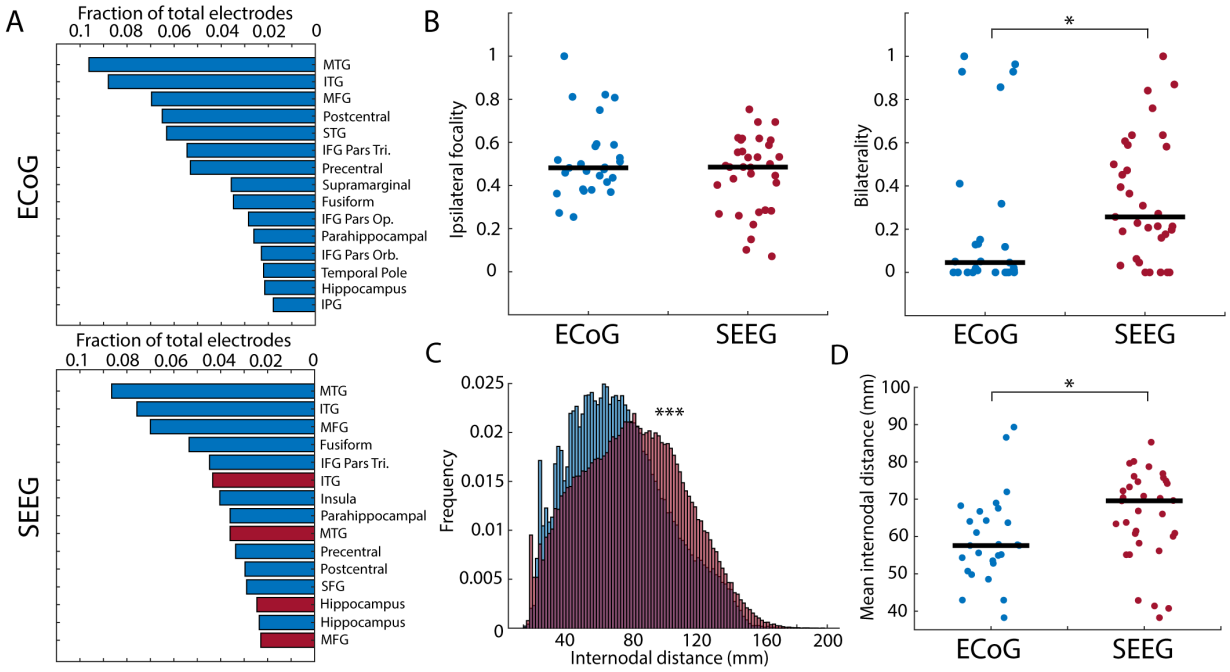

Figure 2. Anatomic distribution of electrodes differs in ECoG and SEEG: (A) Fraction of total electrodes across all patients in ECoG (top) and SEEG (bottom). (B) Ipsilateral focality is not different in ECoG and SEEG (left), but fraction of nodes in hemisphere contralateral to surgical target is higher in SEEG ($p = 0.02$) (right). (C) Differences in distribution of total edges across all patients (Blue: ECoG, Red: SEEG; $p < 0.001$). (D) SEEG patients have a higher average distance between nodes than ECoG patients ($p = 0.01$). MTG: middle temporal gyrus, ITG: inferior temporal gyrus, STG: superior temporal gyrus, MFG: middle frontal gyrus, IFG inferior frontal gyrus, SFG: superior frontal gyrus, IPG = inferior parietal gyrus, * = $p < 0.05$, *** = $p < 0.001$.

distribution of electrode contacts by defining two independent metrics: (i) ipsilateral focality, represented by the fraction of nodes ipsilateral to the resection zone in the same lobe as the primary target, and (ii) bilaterality, defined as the ratio of contralateral to ipsilateral nodes with respect to the resection zone. While there was no significant difference in ipsilateral focality between groups (rank-sum statistic = 853, $p = 0.7$), bilaterality was higher in the SEEG group (rank-sum statistic 673, $p = 0.02$). We then asked whether these anatomical sampling differences affect the distances at which ECoG and SEEG measure connectivity. Histograms of internodal distance (Figure 2C) reveal that ECoG sampling skews towards shorter connections on average compared to SEEG (KS statistic = 0.13, $p < 0.001$). Indeed, at the patient level, SEEG networks also have a higher

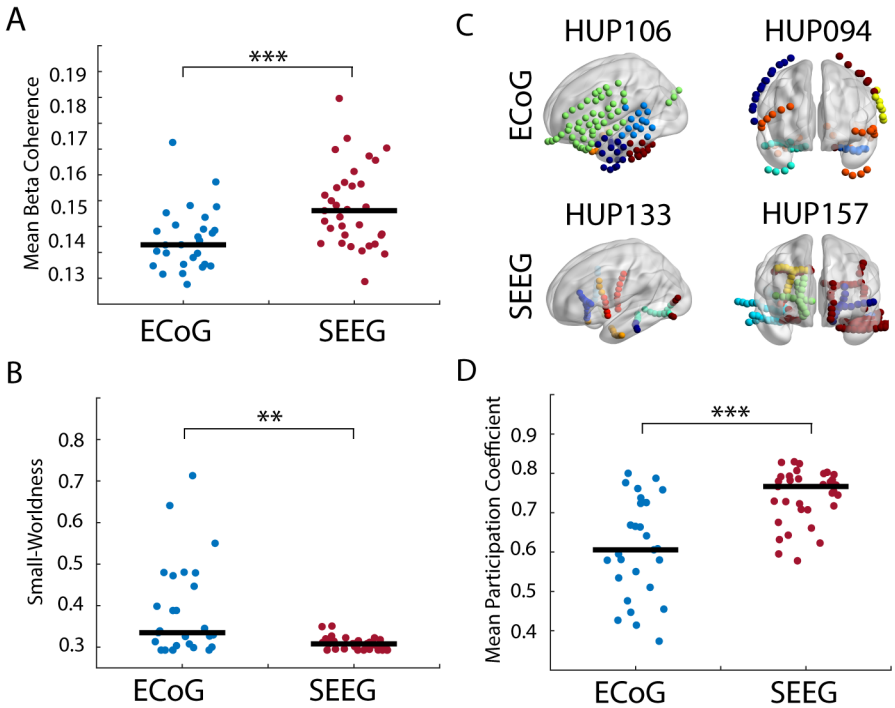

Figure 3: Global network structure is impacted by sampling differences between ECoG and SEEG. (A) Mean connectivity is higher in SEEG compared to ECoG ($p = 9.7e\text{-}4$). (B) ECoG networks have a significantly higher small-world propensity than those mapped by SEEG ($p = 0.003$). (C) One example patient from each modality is shown, node communities are denoted by distinct colors, and node size is scaled by participation coefficient. (D) SEEG nodes (red) have higher average participation coefficient than ECoG ($p = 8.3e\text{-}6$) SEEG. ** = $p < 0.01$, *** = $p < 0.001$.

internodal distance on average (rank-sum statistic = 657, $p = 0.01$). A greater abundance of these longer-distance connections may result in distinct global properties and representations of the epileptogenic zone.

3.2 Differences in spatial sampling affect estimates of network structure

Given the differences in anatomical sampling observed in ECoG and SEEG, we sought to determine whether measures of connectivity and broader network structure differ significantly between groups. Given that we found that SEEG samples brain networks at a longer distance than ECoG, we expected that connectivity strengths in SEEG would be lower compared to ECoG. However, we found a higher mean connectivity as measured by coherence in the beta band (15-40 Hz) in the SEEG group (rank-sum statistic = 601, $p < 0.001$). We then sought to determine whether

observed differences in connectivity, distance, and anatomical distribution affected meso-scale properties of sampled brain networks (Figure 3B). We found that networks sampled by ECoG have higher small-world propensity than those from SEEG (rank-sum statistic = 1027, $p = 0.003$). We finally sought to determine the effect on network modular structure. We probed broader network structure using network modularity to detect nodal communities and display a two example map of communities color-coded by module for patients in the ECoG and SEEG groups (Figure 3C). From these communities, we find a higher mean participation coefficient in SEEG networks compared to ECoG (rank-sum statistic = 601, $p < 0.001$), suggesting a higher integration of discrete clusters of connectivity within broader brain (SEEG) networks (Figure 3D). We next hypothesized that differences in these properties, which describe the meso-scale and global structure of measured brain networks, may alter the ability of graph metrics to uncover pathologic regions.

3.3 Distinct properties of the epileptogenic zone

To this point, we have demonstrated differences in the ways that ECoG and SEEG represent brain networks. We next investigated how these differences both present challenges and opportunities to advance applying graph theory to localize the epileptogenic zone (EZ). We compared the properties of the resection zone, a proxy for the epileptogenic zone, between both ECoG and SEEG using the distinguishability statistic. We show the process for calculating distinguishability in Figure 4A, in which D_{rs} of the strength of resected and spared nodes is calculated as the normalized U-statistic which quantifies the AUC for classifying these two node types. We performed this analysis under several conditions to attempt to account for sampling bias (Supplemental figure 1): (i) 'base' networks with all non-artifact nodes included, (ii) networks with all white matter nodes removed, (iii) networks reduced to a 'minimum ROI' representation where each brain atlas region has one node representing the average of all nodes within that region,

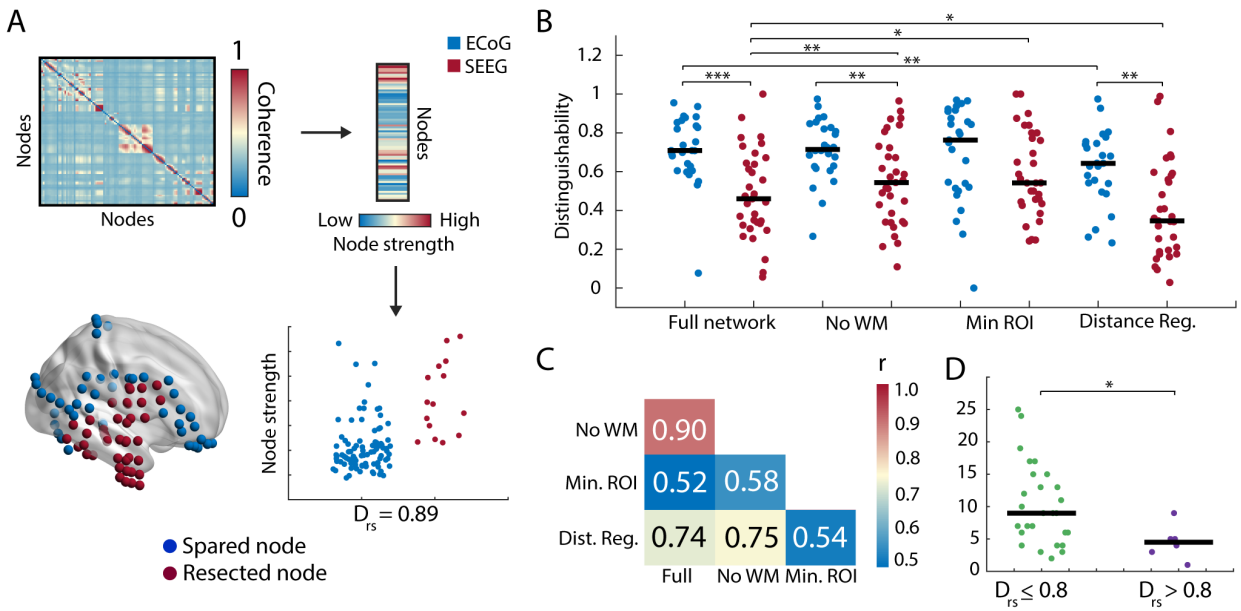

Figure 4: ECoG and SEEG have distinct representations of the epileptogenic zone. (A) We calculated the distinguishability statistic for the resection zone to quantify how well we can determine epileptogenic regions. (B) We found significantly higher distinguishability for ECoG networks compared to SEEG regardless of how networks were adjusted. (Full network: p = 0.0001, no WM: p = 0.003, min ROI: 0.054, Distreg: 0.0013). Regressing out the effects of distance decreased performance in ECoG patients (Full network versus ECoG dist. reg. p = 0.0049). However, eliminating white matter and reducing networks to one node per ROI marginally improved performance in SEEG (SEEG base versus SEEG no WM 0.001, SEEG base versus min ROI 0.011, SEEG base versus distreg 0.12). (C) Correlations in distinguishability across patients with SEEG under different network conditions (D) The number of nodes resected or ablated in surgery was different for patients which achieved good performance (D_{rs} >0.8) versus those that did not (p = 0.023). * = p < 0.05, ** = p < 0.01, *** = p < 0.001.

and (iv) networks in which internodal distance has been regressed out. We performed this process in a previously-reported manner[29] by fitting a two-term rational polynomial (rat11 in MATLAB) to the distance-connectivity data and creating new adjacency matrices that were the residual between the base network and the expected connectivity matrix based on internodal distance in that patient.

From our calculations of D_{rs} we found a substantial disparity in the ability for node strength to distinguish nodes that make up the epileptogenic zone in SEEG compared to ECoG (Figure 4B). This finding persisted under different network conditions beyond full networks (rank-sum = 1084,

p = 0.001), including those with WM removed (rank-sum static = 1023, p = 0.003), and distance regression (rank-sum statistic = 1012, p = 0.005). However, using only one node per ROI yielded performance in ECoG and SEEG that was not significantly different (rank-sum statistic = 954, p = 0.054). In ECoG, the observed high level of D_{rs} under implies that a high node strength accurately identifies EZ nodes compared to the rest of the network. When modifying the network in ECoG, removing the few existing WM nodes and reducing the networks to minimum ROI representations had little change on localization (signed-rank statistic = 108, p = 0.3 and signed-rank statistic = 202, p = 0.7 respectively). Interestingly, regressing out the effect of distance worsened performance contrary to previously published studies (signed-rank static = 323, p = 0.001).

In patients with SEEG, modifying networks by removing WM nodes and reducing networks to a minimum ROI representation improved performance statistically (signed-rank statistic = 96, $p < 0.001$ and signed-rank statistic = 129, p = 0.01, respectively). Furthermore, the poor overall performance of node strength in patients with SEEG was due to many patients having an epileptogenic zone with weak connectivity ($D_{rs} < 0.5$). To investigate reasons for the wide variety in D_{rs} values, we divided the results into patients which had an acceptably high level of D_{rs} which we set at > 0.8 which represents good classifier performance and those for which node strength likely does not provide enough value to be clinically meaningful ($D_{rs} \leq 0.8$). Six patients surpassed this threshold based on minimum ROI distinguishability while 27 did not. We found an association with number of nodes targeted by surgery, with low numbers of nodes being more distinguishable (rank-sum statistic = 53, p = 0.02). However, there was no association with total number of network nodes (rank-sum statistic = 69), surgical outcome (chi-square test, p = 0.4), or the region of primary target (chi-square test, p = 0.6). The variability in SEEG introduces a

complex relationship between observed pathology and functional connectivity, however modifying networks to correct for sampling bias may improve the utility of network models.

4. Discussion:

Understanding the sampling differences of different iEEG approaches is critically important when applying network models to interpret intracranial data. Here, we show stereotyped differences in anatomic electrode distributions in ECoG and SEEG, and demonstrate how these different approaches to spatial sampling affect measures of a network's strength and structure. To illustrate the significance of these differences, we assess how well connectivity can distinguish between epileptogenic and non-epileptogenic regions as mapped by ECoG versus SEEG. We show that node strength, a frequently studied network metric in epilepsy, often fails to accurately localize the epileptogenic zone in patients implanted with SEEG, and we provide several potential explanations and methods for partially mitigating this disparity.

Despite relatively similar distributions in ultimate surgical targets, we found a clear differences in anatomical locations of SEEG electrode contacts compared to ECoG. The most significant of these were that SEEG has a greater level of bilaterality which makes sense as SEEG is more frequently used to sample interhemispheric connections in our center. The ability to place each depth electrode independently results in coverage that may be more customized to each patient's specific clinical scenario and more variable across patients in SEEG compared to ECoG[34]. Electrodes contralateral to the ultimate site of resection were placed for the clinical purpose of lateralization[35] rather than to quantify network connectivity, and these nodes likely contribute to a significant portion of the differences between iEEG modalities given that bilateral implants are less common and often precluded in ECoG because of the risk of morbidity and surgical complications.

Our finding that SEEG patients have higher mean connectivity despite a higher mean internodal distance compared to ECoG is unexpected in the context of the well-documented inverse relationship between connectivity and distance. However, one possible explanation is the hardware itself: each SEEG electrode has multiple contacts along the same lead at different depths, often in a single gyrus, which could allow for volume conduction to create artificially high connectivity. This same principle applies to electrodes in contiguous white matter structures along single Stereo EEG electrodes. Furthermore, the different physical size and cylindrical shape of each electrode contact in SEEG compared to ECoG records local fields from different types of neural populations which could have distinct coherence values. Finally, the guiding principle of SEEG is to target network regions known to be functionally connected to each other, for example multiple structures in the limbic or default mode networks, which could also result in high measured connectivity despite a higher internodal distance, in addition to the higher observed network integration that is fundamental to SEEG technique. While previous studies have found superior prediction of surgical outcome after correcting for the connectivity – distance relationship, it may be important to perform this process separately for depth and cortical electrodes in the context of our results.

From the differences in network representation between ECoG and SEEG we found that the ability to localize the epileptogenic zone differs between these techniques. In ECoG, the majority of patients had $D_{rs} > 0.5$, indicating that the epileptogenic zone could be identified by targeting high-strength nodes. Meanwhile, D_{rs} values of SEEG revealed that the epileptogenic zone could have nearly any value of node strength compared to the rest of the network, resulting in negligible distinguishability at the group level. The finding that the surgical targets can be more easily distinguished by node strength in ECoG compared to SEEG may reflect the distinct

philosophies underlying these strategies. More importantly, this difference likely also reflects significant selection bias, in that ECoG is usually reserved for patients in whom localization of seizures to a particular cortical surface region is to be performed, often within a single lobe or contiguous region. This is different than SEEG, which can be applied more broadly to patients who do not meet these criteria, many of whom were previously not candidates for ECoG because of suspected deep sources or widely distributed epileptic networks. Subdural grids historically were used to delineate the boundaries of an epileptogenic region for subsequent resection[1]. These grids, with regular interelectrode spacing, result in similar local sampling around each individual contact, and perhaps are more sensitive to differences in connectivity that result from local pathology. For SEEG, the irregular sampling of a combination of cortical and deeper structures is more likely to record a heterogeneous network in which high node strengths could potentially be a function more of electrode placement than pathology. Thus, simple metrics such as node strength which do not account for the topology of the brain's underlying connectivity may not be able to localize the EZ reliably in SEEG, despite efforts to constrain the problem or modify networks to partially correct for sampling bias. It is interesting, however, that constraining SEEG networks to represent connections between specific anatomic structures rather than individual contacts, which is an important tenant of SEEG targeting, and the basis of interventions based upon SEEG, significantly improved localization performance to a level close to that of ECoG. Future studies could potentially aggregate connectivity across patients, and form a template of inter-regional intracranial EEG from which individual edge weights could be tested against the same connections at the population level, thus avoiding the limitations of node strength's sampling bias. Aggregating large numbers of patients to map these patterns across specific epilepsy types, linked closely to

anatomical localization of networks, is a new and important area of focus for our group, motivated by our findings.

Our study adds to the growing body of literature on methodological considerations for applying network models clinically[22]. From these studies, we recognize that a major challenge in applying network models to epileptic brain is determining whether observed patterns in brain activity and network structure truly capture the phenomena of interest, and to what extent they arise from sampling artifact. To this end, we must acknowledge that the sampling bias in both ECoG and SEEG is distinct, and that subtle differences in the arrangement of electrodes can determine whether connectivity can accurately uncover true pathology. This sampling bias is more complex than just whether or not a particular target was sampled, as the signal from important targets must be significantly above the "noise." Distinct differences in surgical practice and the relative paucity of data sharing has previously hampered uncovering the differences between ECoG and SEEG, however our study and sharing of a large, multicenter dataset will mark significant progress towards these goals.

A natural extension of our work here is to ask whether localization models that use interictal iEEG are fit for clinical translation given the wide-reaching effects of differences in spatial sampling. Indeed, a host of approaches favor imaging-derived connectivity applied to both graph theory and phenomenological neural mass modeling[34] wherein the effects of sampling are less significant. Many of these approaches have revealed capability in localizing the epileptogenic zone[35]. One of them, based upon the Epileptor model[36], is currently undergoing clinical studies. However, despite the advantages of imaging in the spatial domain, the real-time nature of iEEG, the ability to associate interictal networks directly with seizure recordings, as well as the ability to perturb network dynamics by stimulation merit further study of interical iEEG. Ultimately, the

best approach will likely unite information from both invasive and non-invasive methods. Such studies on structure-function correlation are an active area of research,[37] and future studies are needed to localize the EZ with multimodal approaches so that all useful information can be leveraged while minimizing the effects of sampling.

Despite its encouraging results in illuminating the differences between ECoG and SEEG networks, our study has several key limitations. One is that while the graph metric we chose for localization, node strength, is frequently studied in patients with epilepsy, other metrics and models might have revealed a different relationship between findings in ECoG and SEEG. However, given that node strength is among the least sensitive network metrics to sampling bias[22], we felt that it was a reasonable choice to compare these approaches. Another key limitation is that we could not balance SEEG and ECoG groups for surgical type due to clinical practice at our center. Indeed, some of the decreased performance of EZ localization seen in SEEG compared to ECoG may be accounted for by the lower number of targeted nodes amongst a higher number of total nodes in the SEEG group.

Ultimately, clinical judgement of risk and reward will drive the choice between ECoG and SEEG for individual patients. While the path of clinical translation for network models is complicated by inherent sampling biases across techniques and varying surgical practice among institutions, we believe it is vital to study SEEG more carefully, in addition to ECoG networks, to match the global trend towards SEEG. We hope that our results, data, and code will accelerate research to build practical quantitative tools to guide invasive epilepsy therapy, and to sharing and aggregating data across centers. Finally, we believe that carefully understanding the sampling properties of networks mapped by intracranial EEG can extend the use of graph theory to broader problems in translational human neuroscience. Many studies in this realm are currently being

conducted in implanted epilepsy patients while they wait to have seizures in hospital. In the not too distant future it is likely that this group will expand dramatically to patients implanted with ambulatory iEEG recording and stimulation devices for diagnosis and treatment of a wide variety of neurological and psychiatric conditions.

5. Acknowledgements:

J.B. acknowledges funding from NIH 6T32NS091006. B.L. acknowledges funding from the Pennsylvania Tobacco Fund, NINDS R01: R01NS099348, the Mirowski Family Foundation, Jonathan Rothberg, and Neil and Barbara Smit. K.A.D acknowledges funding from NINDS K23: NS092973 and the Thornton Foundation.

6. Competing interests:

The authors report no relevant disclosures.

7. References:

1. Lüders, H. O., Najm, I., Nair, D., Widdess-Walsh, P. & Bingman, W. *Definition and localization of the epileptogenic zone The epileptogenic zone: general principles*.
2. Reif, P. S., Strzelczyk, A. & Rosenow, F. The history of invasive EEG evaluation in epilepsy patients. *Seizure* **41,** 191–195 (2016).
3. Jehi, L. *The Epileptogenic Zone: Concept and Definition*.
4. Youngerman, B. E., Khan, F. A. & McKhann, G. M. Stereoelectroencephalography in epilepsy, cognitive neurophysiology, and psychiatric disease: Safety, efficacy, and place in therapy. *Neuropsychiatric Disease and Treatment* **15,** 1701–1716 (2019).
5. Parvizi, J. & Kastner, S. Human Intracranial EEG: Promises and Limitations. doi:10.1038/s41593-018-0108-2
6. Téllez-Zenteno, J. F., Ronquillo, L. H., Moien-Afshari, F. & Wiebe, S. Surgical outcomes in lesional and non-lesional epilepsy: A systematic review and meta-analysis. *Epilepsy Res.* **89,** 310–318 (2010).
7. Neuroscientist, C., Kramer, M. A. & Cash, S. S. Overview of Epilepsy and Seizures, Rhythms, and Networks Different Kinds of Seizures and Implications for Spatial Characterization of Epilepsy Epilepsy as a Disorder of Cortical Network Organization. *Neurosci.* **18,** 360–372 (2012).
8. Bernhardt, B. C., Bonilha, L. & Gross, D. W. Network analysis for a network disorder: The emerging role of graph theory in the study of epilepsy. *Epilepsy and Behavior* **50,** (2015).
9. Bassett, D. S., Zurn, P. & Gold, J. I. On the nature and use of models in network neuroscience. *Nat. Rev. Neurosci.* (2018). doi:10.1038/s41583-018-0038-8

10. Shah, P. *et al.* High interictal connectivity within the resection zone is associated with favorable post-surgical outcomes in focal epilepsy patients. *NeuroImage Clin.* 101908 (2019). doi:10.1016/J.NICL.2019.101908
11. Sinha, N. *et al.* Predicting neurosurgical outcomes in focal epilepsy patients using computational modelling. *Brain* (2017). doi:10.1093/aww332
12. Lagarde, S. *et al.* Interictal stereotactic-EEG functional connectivity in refractory focal epilepsies. *Brain* **141,** 2966–2980 (2018).
13. Goodfellow, M. *et al.* Estimation of brain network ictogenicity predicts outcome from epilepsy surgery. *Sci. Rep.* **6,** 29215 (2016).
14. Kini, L. G. *et al.* Virtual resection predicts surgical outcome for drug-resistant epilepsy. *Brain* (2019). doi:10.1093/brain/awz303
15. Khambhati, A. N., Davis, K. A., Lucas, T. H., Litt, B. & Bassett, D. S. Virtual Cortical Resection Reveals Push-Pull Network Control Preceding Seizure Evolution. *Neuron* (2016). doi:10.1016/j.neuron.2016.07.039
16. Khambhati, A. N. *et al.* Dynamic Network Drivers of Seizure Generation, Propagation and Termination in Human Neocortical Epilepsy. *PLOS Comput. Biol.* **11,** e1004608 (2015).
17. Panzica, F., Varotto, G., Rotondi, F., Spreafico, R. & Franceschetti, S. Identification of the Epileptogenic Zone from Stereo-EEG Signals: A Connectivity-Graph Theory Approach. *Front. Neurol.* **4,** 175 (2013).
18. Pizzo, F. *et al.* Epileptogenic networks in nodular heterotopia: A stereoelectroencephalography study. *Epilepsia* **58,** 2112–2123 (2017).
19. Wilke, C., Worrell, G. & He, B. Graph analysis of epileptogenic networks in human partial epilepsy. *Epilepsia* **52,** 84–93 (2011).
20. Cruzat, J. *et al.* The dynamics of human cognition: Increasing global integration coupled with decreasing segregation found using iEEG. *Neuroimage* **172,** 492–505 (2018).
21. Buch, V. P. *et al.* Network Brain-Computer Interface (nBCI): An Alternative Approach for Cognitive Prosthetics. (2018). doi:10.3389/fnins.2018.00790
22. Conrad, E. C. *et al.* The sensitivity of network statistics to incomplete electrode sampling on intracranial EEG. (2020). doi:10.1162/netn_a_00131
23. Katz, J. S. & Abel, T. J. Stereoelectroencephalography Versus Subdural Electrodes for Localization of the Epileptogenic Zone: What Is the Evidence? *Neurotherapeutics* (2019). doi:10.1007/s13311-018-00703-2
24. Wagenaar, J. B., Brinkmann, B. H., Ives, Z., Worrell, G. A. & Litt, B. A multimodal platform for cloud-based collaborative research. in *2013 6th International IEEE/EMBS Conference on Neural Engineering (NER)* 1386–1389 (IEEE, 2013). doi:10.1109/NER.2013.6696201
25. Kini, L. G., Davis, K. A., Wagenaar, J. B. & Davis@uphs, K. Data integration: Combined Imaging and Electrophysiology data in the cloud. *Neuroimage* (2016). doi:10.1016/j.neuroimage.2015.05.075
26. Azarion, A. A. *et al.* An open-source automated platform for three-dimensional visualization of subdural electrodes using CT-MRI coregistration. *Epilepsia* **55,** 2028–2037 (2014).
27. Yushkevich, P. A. *et al.* User-guided 3D active contour segmentation of anatomical structures: Significantly improved efficiency and reliability. *Neuroimage* **31,** 1116–1128 (2006).

28. Tzourio-Mazoyer, N. *et al.* Automated Anatomical Labeling of Activations in SPM Using a Macroscopic Anatomical Parcellation of the MNI MRI Single-Subject Brain. *Neuroimage* **15,** 273–289 (2002).
29. Wang, Y. *et al.* Interictal intracranial electroencephalography for predicting surgical success: The importance of space and time. *Epilepsia* epi.16580 (2020). doi:10.1111/epi.16580
30. Newman, M. E. J. Modularity and community structure in networks. *Proc. Natl. Acad. Sci. U. S. A.* **103,** 8577–8582 (2006).
31. Guimerà, R. & Nunes Amaral, L. A. Cartography of complex networks: modules and universal roles. *J. Stat. Mech. Theory Exp.* **2005,** P02001-1 (2005).
32. Bassett, D. S. & Bullmore, E. T. Small-World Brain Networks Revisited. *Neuroscientist* **23,** 499–516 (2017).
33. Muldoon, S. F., Bridgeford, E. W. & Bassett, D. S. Small-world propensity and weighted brain networks. *Sci. Rep.* **6,** 1–13 (2016).
34. Jirsa, V. K. *et al.* The Virtual Epileptic Patient: Individualized whole-brain models of epilepsy spread. *Neuroimage* **145,** 377–388 (2017).
35. Proix, T. E., Bartolomei, F., Guye, M. & Jirsa, V. K. Individual brain structure and modelling predict seizure propagation. *Brain* 641–654 (2017). doi:10.1093/awx018
36. Jirsa, V. K., Stacey, W. C., Quilichini, P. P., Ivanov, A. I. & Bernard, C. On the nature of seizure dynamics. *A J. Neurol.* doi:10.1093/brain/awu147
37. Shah, P. *et al.* Characterizing the role of the structural connectome in seizure dynamics. *Brain* **142,** 1955–1972 (2019).